RESEARCH ARTICLE

Simulation of fire exposure behavior to building structural elements using LISA FEA V.8.

ACO WAHYUDI EFENDI [1]

[1] *Student of the Civil Engineering Doctoral Degree Study Program, Universitas Sebelas Maret, Indonesia*

Corresponding author's email: acowahyudiefendi@student.uns.ac.id

Abstract

The purpose of this work is to evaluate the most generally used techniques for measuring the thermal conductivity of concrete, as well as to consider the variables influencing the thermal conductivity of cement-based materials. Based on previous research indicating that the pattern of heat flow can be modeled in a numerical analysis program and provide a hue of coverage and differences in indoor temperature conditions, as well as the impact that occurs on several elements in the room, a heat simulation analysis was performed in this study due to a fire.

The researchers in this study simulated the flow pattern from the temperature that occurred due to fire in a room measuring 4000x4000 mm with a wall thickness of 200 mm with Hebel/light brick material, floor plate thickness was 120 mm, and the size of the building column structural elements was 400x400 mm with the material reinforced concrete.

According to the simulation results of a fire that occurred in the middle of the room with two conditions for installing hebel walls, namely covering the building structure columns and those behind the building structure columns, there is an increase in the temperature of the column with a ratio of 1.062 in the two conditions where the temperature of the wall lining the column is 6.28% lower than the temperature of the wall behind the column, while the heat flux magnitude that occurs is lower.

Keyword: Conductivity, FEM, Fire, Heat, LISA, Thermal

Introduction

In both industrial and residential heating applications, heat transmission from the flame of a hollow plate burner impinging on a flat plate is significant. This research takes into account inline, star, and staggered hole layouts with three different lengths between holes. Over the whole mix flow range evaluated in this study, the intermediate pitch of 7 mm is the best pitch.(Hindasageri et al., 2015). The heat transfer calculation in a torch furnace is presented as an example, and it is noticeably non-uniform in nature. Calculations show that a new furnace is needed to reduce ingot heating non-uniformity, improve fuel rate, and enhance furnace capacity.(Makarov, 2016).

The temperature at the joints on the open side of the sandwich panel is initially lower than that of the panel, according to the fire test findings. Because of the significant radiation in the gap, the joint temperature rises much faster than the panel temperature. A joint gap of 10 mm or larger will result in a substantially higher joint temperature than the panel temperature, resulting in a sandwich panel system insulation performance of less than 60 minutes, even though the panels may be able to meet a far longer standard fire resistance level.(Wang & Foster, 2017).

When assessing the quantity of heat transmission by conduction, the thermal conductivity of cement-based materials such as concrete is an essential aspect. Thermal conductivity is affected by moisture content, temperature, aggregate type, cementitious material type, and concrete density. The purpose of this work is to evaluate the most generally used techniques for measuring the thermal conductivity of concrete, as well as to consider the variables influencing the thermal conductivity of cement-based materials. In addition, based on data supplied by academics, this study proposes a generic equation for forecasting the heat conductivity of concrete.(E. Asadi, 2018).

Based on previous research indicating that the pattern of heat flow can be modeled in a numerical analysis program and provide a hue of coverage and differences in indoor temperature conditions, as well as the impact that occurs on several elements in the room, a heat simulation analysis was performed in this study due to a fire. It is envisaged that by utilizing a wall material in the form of light brick concrete and a distinct wall layout pattern indoors, it would be possible to convey information about the color of heat flow that influences the column structure in the room .

Methods

A. Heat Transfer

Heat transfer is a vector quantity that takes place via conduction, convection, and radiation. Conductive heat transmission in solids is a combination of molecular vibrations and free electron energy transport. Thermal conductivity (k-value) is a characteristic of a substance that displays its capacity to conduct heat. Building energy consumption is determined by the thermal conductivity characteristics of the building materials. Mineral wool (0.03-0.04 W/m.°K), cellulose insulation (0.04-0.05 W/m.°K), cork (0.04-0.05 W/m.°K), expanded polystyrene (EPS) (0.03-0.04 W/m.°K), polyurethane (0.02-0.03 W/m.°K), wood (0.14 W/m.°K), and ceramic tiles (1.10 W/m.°K) can minimize energy consumption in buildings. (I. Asadi et al., 2018).

It is important to use an accurate method for measuring the thermal conductivity of concrete in order to calculate the energy consumption of buildings. Furthermore, it should be mentioned that the k-value of concrete is affected by a number of elements. The impact of each component on the thermal conductivity of concrete is discussed in this review. Considering these elements during concrete casting and using concrete in buildings can result in more energy-efficient and sustainable structures.

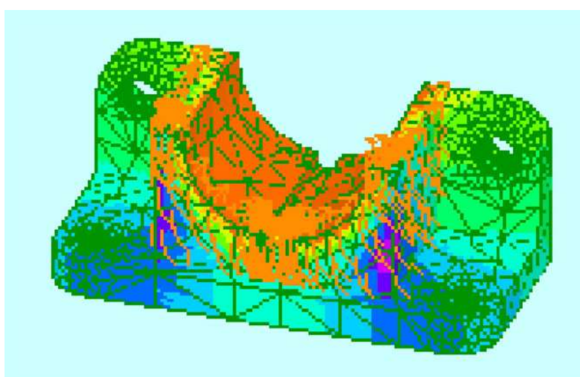

Figure 1. Heat transfer modeling (LISA)

B. Concrete Thermal Conductivity Measurement Methods

Thermal conductivity is a material attribute that pertains to heat conduction. The thermal conductivity of a porous material is determined by the thermal conductivity of the fluid phase and the thermal conductivity of the solid phase. Some techniques for measuring the thermal conductivity of porous materials include two linear parallel probes, a plane heat source, and a heated guarded plate.

C. Hebel Brick Mechanical Properties

Hebel brick is a material that mimics concrete and has the attributes of strength, lightweight, economy, size uniformity, soundproof, durability, heat resistance, fire resistance, and environmental friendliness. Hebel bricks are available in a variety of sizes, with lengths of 600 mm and heights of 200 mm, as well as thicknesses of 75, 100, 125, 150, 175 and 200 mm. Hebel brick mechanical characteristics include strength and compressive strength, with EBH = elastic modulus of Hebel bricks (MPa), f'BH = compressive strength of Hebel bricks (MPa), f'vH = shear strength horizontal hebel masonry (MPa), P = maximum load (N), and A = compression area (mm^2), Pu = maximum shear load (N), W = tool mass (N), wb = width of Hebel bricks, hb = length of compression area/Hebel bricks (mm), h = length of shear plane (mm), Wc = unit weight of Hebel Bricks by volume (kg/m^3).

The destructive test method was used to determine the mechanical characteristics of hebel bricks. Hebel brick size in crushing strength test (f'BH) has dimensions of 100 mm x 100 mm x 100 mm and is tested using a Compression Testing Machine, whereas Hebel brick size in shear strength test (f'vH) has dimensions of 300 mm x 200 mm and is tested using a Compression Testing Machine (CTM). (Ahmad Zarkasi, 2021).

D. Finite element method (FEM)

The finite element method uses an utilizes a component discretization way to deal with tackle the issue of tracking down relocations of vertices/associations/grids and primary powers. Discrete component conditions are connected with the lattice technique for primary examination and the outcomes got are indistinguishable from those of traditional investigation for structures. The discretization should be possible with one-layered components , two-layered or three-layered . This approach utilizes a continuum component to decide an answer that is nearer to reality. (Albahkali et al., 2021; Chen et al., 2021; D’Aniello, 2017; A. W. Efendi, 2022c, 2022a, 2022b, 2022d; Elsanadedy et al., 2021; Gullett et al., 2020; Okafor et al., 2020; Song et al., 2017).

E. LISA FEA

LISA, a well known limited component examination application, was utilized to gauge the temperature climb for three distinct models of intensity exchangers. For line component models just, the convection coefficient of the baseplate surface not set in stone as a portion of the worth utilized somewhere else since we can't bar convection from gathering the baseplate surface with the face determination device. For the other two models, it's not difficult to prohibit the mounting surface from convection - we simply don't choose that surface. (Akcay et al., 2021; A. W. Efendi, 2022c, 2022b, 2022e; A. W. Efendi et al., 2022, 2022; EFENDI, 2022; I. A. W. Efendi, 2022; Fumagalli et al., 2022; Qian, 2022).

Results and Discussion

The researchers in this study simulated the flow pattern from the temperature that occurred due to fire in a room measuring 4000x4000 mm with a wall thickness of 200 mm with Hebel/light brick material, floor plate thickness was 120 mm, and the size of the building column structural elements was 400x400 mm with the material reinforced concrete, as shown in Figure 2.

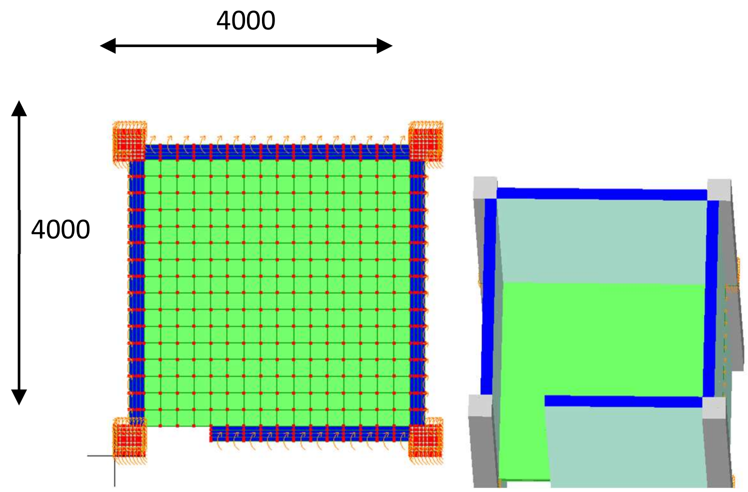

Figure 2. Room modeling (LISA, 2023)

Based on the experimental study that has been conducted, for the material characteristics mentioned in table 1 and 2.

Table 1. Material Data

No.	Type materials	Parameter	Symbol	Value
1	PK concrete	concrete compressive strength	f'c	21,21 MPa
	(a)	Elasticity Modulus	Ec	20.336,91 MPa
		Poisson's rasio	Vc	0,18
2	Reinforcing steel	Yield Stress	fy	421,57 MPa
	P.10	Elasticity Modulus	Es	166.785,44 MPa
		Poisson's rasio	Vs	0,30
3	Reinforcing steel	Yield Stress	fy	340,56 MPa
	P.8	Elasticity Modulus	Es	163.132,88 MPa
		Poisson's rasio	Vs	0,30
		concrete compressive strength	fB	2,23 MPa
4	Hebel Wall	Elasticity Modulus	EB	1.119,47 MPa
		Poisson's rasio	VB	0,15 (Chen, 2003 in
		concrete compressive strength	fB	Dewi, 2012)

Source: (Ahmad Zarkasi, 2021)

Table 2. Thermal Conductivity Material

Material	Young Modulus (N/mm^2)	Density (N/mm^3)	Poison Rasio	Thermal Conductivity W/mm °C
Steel	210000	0.0000785	0.3	0.043
Concrete	210000	0.0000229	0.2	0.00092
Wood	210000	0.0000098	0.3	0.00017
Hebel	1.119,47	0.0000119	0.15	0.00042

Source: (I. Asadi et al., 2018)

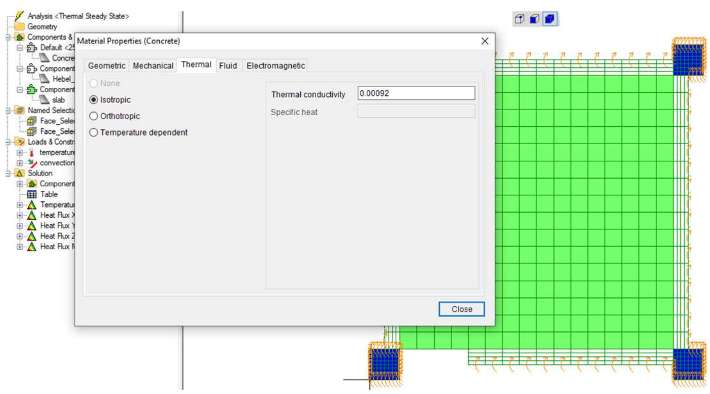

Figure 3. Thermal conductivity of concrete in colomn (LISA, 2023)

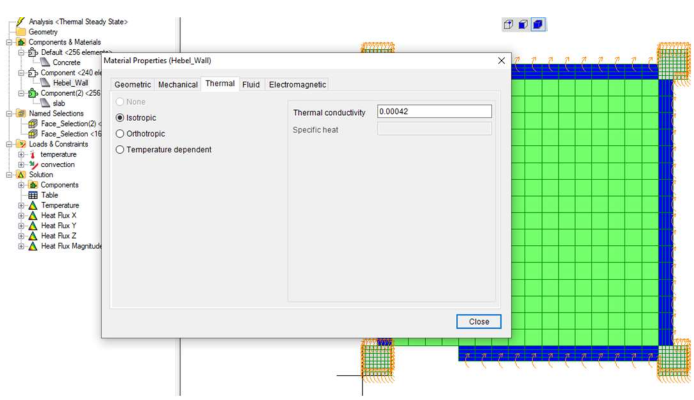

Figure 4. Thermal conductivity of hebel wall (LISA, 2023)

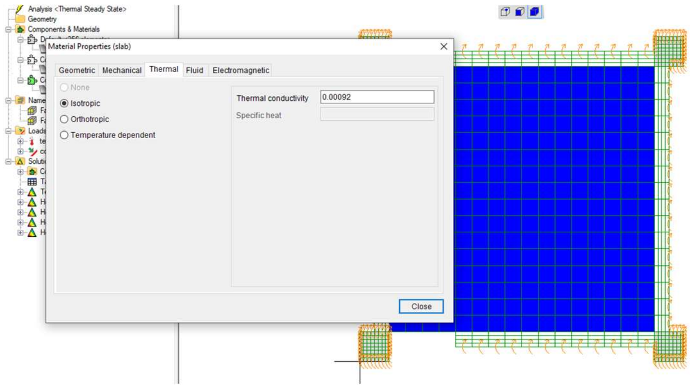

Figure 5. Thermal conductivity of concrete in floor (LISA, 2023)

The observed behavior can be utilized as a reference if a concrete building structure is burning at temperatures of up to 900°C or higher and for a period of up to 7 hours or longer shown in figure 6. Concrete is a type of construction material, it is more resistant to fire and heat than other materials such as wood or steel. This is due to the fact that concrete is a poor heat conductor. When unfired concrete is fired at 300 degrees Celsius, no noticeable changes occur, but as the temperature rises, the reduction becomes apparent. (A. W. Efendi, 2022b; Trisni Bayuasri et al., 2006)

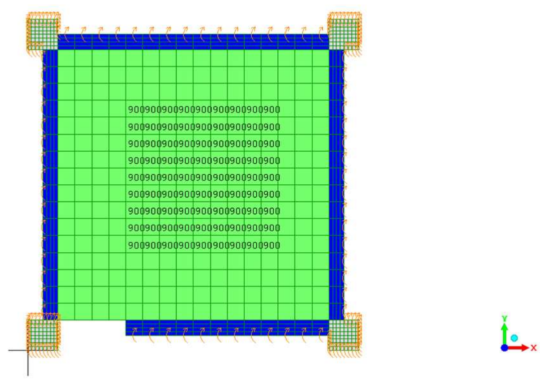

Figure 6. Thermal conductivity of concrete in floor (LISA, 2023)

Figure 7 shows the characteristics with an ambient room temperature of 22 degrees Celsius and a heat transfer coefficient of 400.

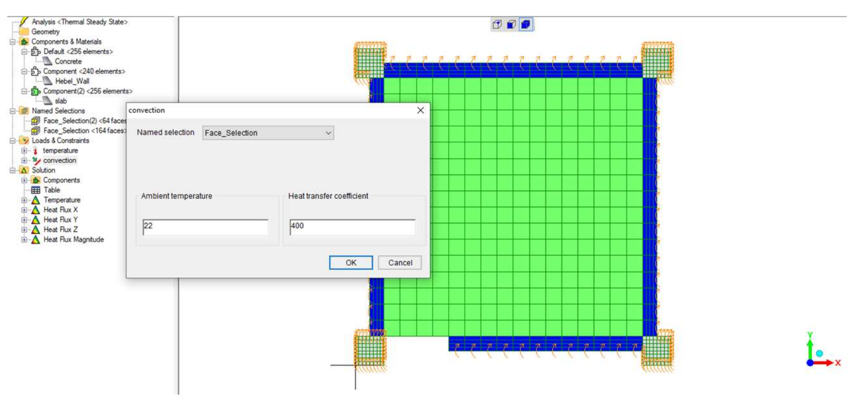

Figure 7. Convection paramater (LISA, 2023)

A. Fire simulation with linked walls covering the columnar structural components in the room.

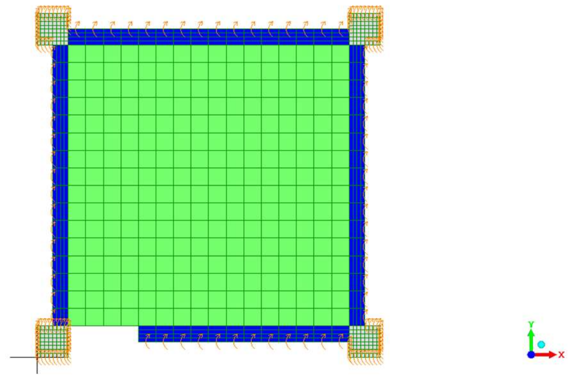

Figure 8. Walls covering the columnar structural (LISA, 2023)

In the first model, a simulation is carried out if the wall is installed to cover the column of the building structure as shown in Figure 8 with the fire point in the middle of the room.

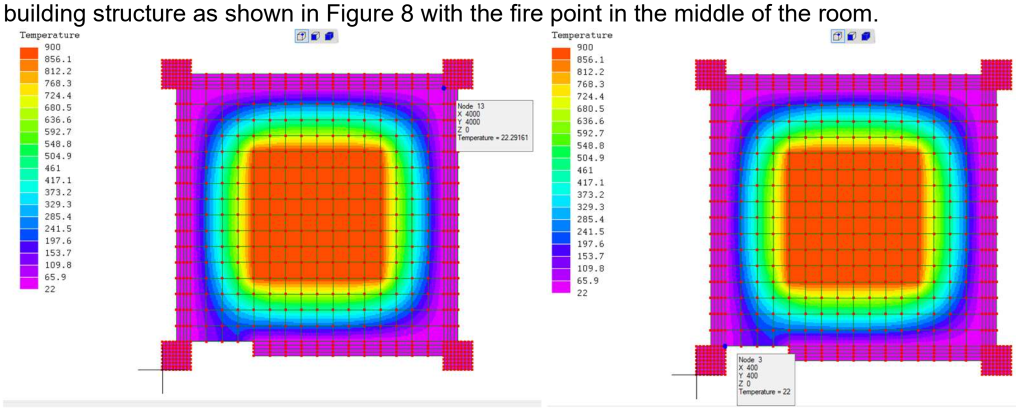

(a) (b)

Figure 9. Simulation results and temperature induced hue due to fire (LISA, 2023)

Figure 9 shows the results of an indoor fire simulation with the effect hue, showing that the temperature value in the middle of the room reaches 900 degrees Celsius, while the temperature drops to only around 22.29 degrees Celsius (a) in the inner column and only 22 degrees Celsius (b) in the outer column near the entrance.

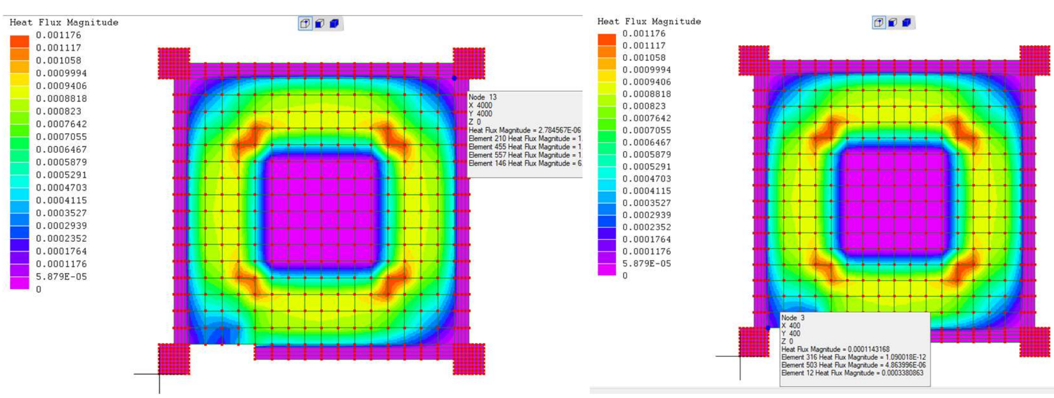

(a) (b)

Figure 10. Simulation results and heat flux magnitude induced hue due to fire (LISA, 2023)

Figure 10 shows the interior column's heat flux magnitude of 0.00000278 W/mm^2(a), whereas the column at the open room door receives a heat flux magnitude of 0.000114 W/mm^2(b).

A. Fire simulation with walls linked to the back side of the room's column structural parts.

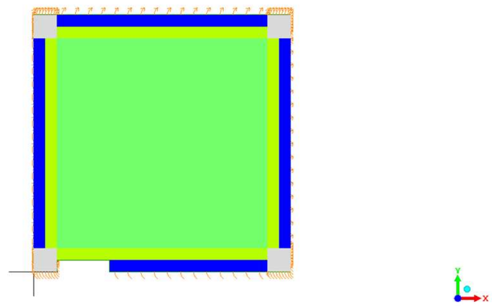

Figure 11. Walls the back side of column structural (LISA, 2023)

In the second model, a simulation is carried out if the wall is installed to back side the column of the building structure as shown in Figure 11 with the fire point in the middle of the room.

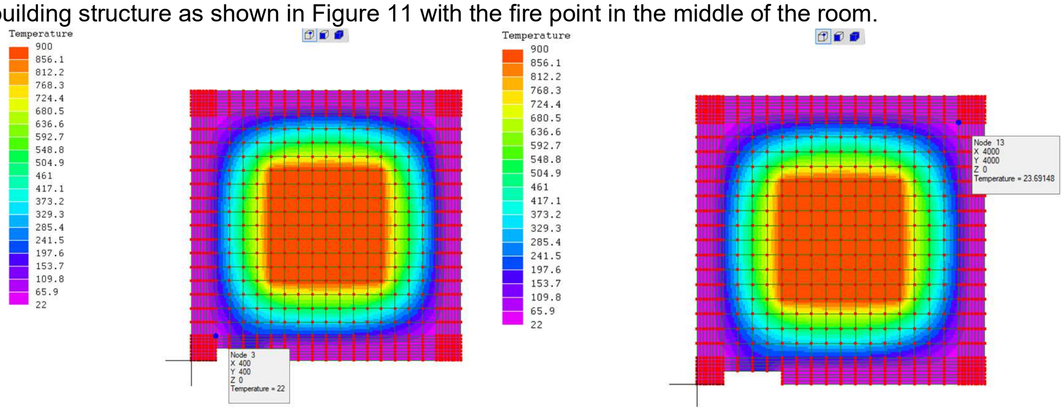

(a) (b)

Figure 12. Simulation results and temperature induced hue due to fire (LISA, 2023)

Figure 12 shows the results of an indoor fire simulation with the effect hue, showing that the temperature value in the middle of the room reaches 900 degrees Celsius, while the temperature drops to only around 23.69 degrees Celsius (a) in the inner column and only 22 degrees Celsius (b) in the outer column near the entrance.

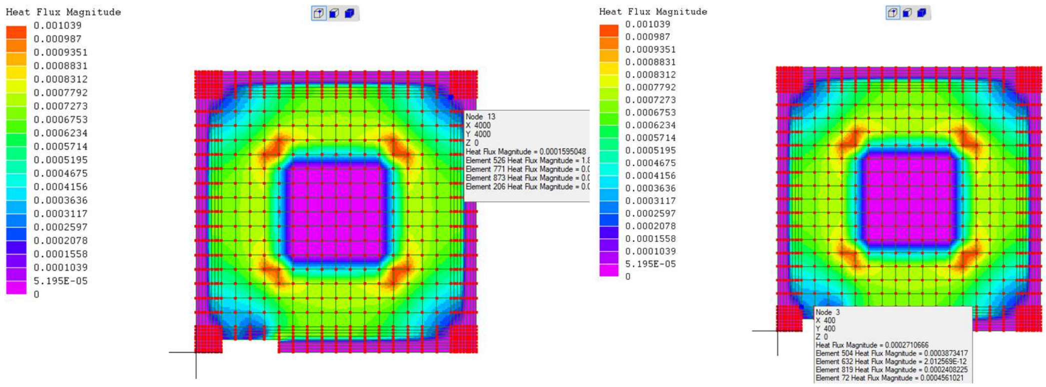

(a) (b)

Figure 13. Simulation results and heat flux magnitude induced hue due to fire (LISA, 2023)

Figure 13 shows the interior column's heat flux magnitude of 0.0001598 W/mm^2(a), whereas the column at the open room door receives a heat flux magnitude of 0.000271 W/mm^2(b).

CONCLUSION

According to the simulation results of a fire that occurred in the middle of the room with two conditions for installing hebel walls, namely covering the building structure columns and those behind the building structure columns, there is an increase in the temperature of the column with a ratio of 1.062 in the two conditions where the temperature of the wall lining the column is 6.28% lower than the temperature of the wall behind the column, while the heat flux magnitude that occurs is lower.

REFERENCE

Ahmad Zarkasi. (2021). PERMODELAN DINDING BATA RINGAN MENGGUNAKAN SOFTWARE SAP 2000 V.18.2. *SIGMA: Jurnal Teknik Sipil*, 12–20.

Akcay, N., Gökalp, A. S., Günlemez, A., & ... (2021). Comparison of LISA vs INSURE Technique Using Nasal Intermittent Positive Pressure Ventilation (NIPPV) Support In Preterm Infants: A Randomized Controlled Trial. *Medical Journal of ….* https://search.ebscohost.com/login.aspx?direct=true\&profile=ehost\&scope=site\&authtype=crawler\&jrnl=13059319\&AN=150026811\&h=oa0JPzH%2F7kU0O6pXKM9bccbhmpQEDKIgq3iXNk0ZUZxlRjSTzIU5R%2BKnLbrndMQP950wl66%2B7Ip5scAz0%2BViPA%3D%3D\&crl=c

Albahkali, T., Alsanabani, N., & ... (2021). A Concept to Estimate the Life Cycle of the Railway Track Using Finite Element Modeling. *… International Journal ….* http://journal.multiphysics.org/index.php/IJM/article/view/762

Asadi, E. (2018). Nonlinear behavior and design of mid- to high-rise diagrid structures in seismic regions. In *Engineering Journal* (Vol. 55, Issue 3, pp. 161–180).

Asadi, I., Shafigh, P., Hassan, Z. F. B. A., & Mahyuddin, N. B. (2018). Thermal conductivity of concrete – A review. *Journal of Building Engineering*, *20*, 81–93. https://doi.org/10.1016/j.jobe.2018.07.002

Burle, C. C. (2022). Effect of Semi Rigid Joints On Design of Steel Structure. *International Journal of Research in Engineering ….*

Chen, X., Pan, L., Xu, L., & Shi, C. (2021). Three-Dimensional Vehicle–Curved Track Dynamic Model Based on FEM and DEM. *… Journal of Structural Stability and ….* https://doi.org/10.1142/S0219455421501790

Costanzo, S., D'Aniello, M., Lorenzo, G. Di, & ... (2019). Seismic design of two-storey X-bracings. *… and Ductility of Steel ….*

D’Aniello, M. (2017). Finite element analyses on free from damage seismic resisting beam-to-column joints. In *COMPDYN 2017—Proceedings of the 6th International Conference on Computational Methods in Structural Dynamics and Earthquake Engineering* (Vol. 1, pp. 802–814). https://doi.org/10.7712/120117.5458.17524

Daudet, L. R., & Nguyen, H. (2018). Drift clip. *US Patent 10,087,617*.

Efendi, A. W. (2022a). ANALISIS PERKUATAN KOLOM PASCA KEBAKARAN PADA GEDUNG DPRD KALIMANTAN TIMUR. *JURNAL RIVET*. http://jurnal.unidha.ac.id/index.php/RIVT/article/view/412

Efendi, A. W. (2022b). Behavior Analysis of Building Structures After a Fire with FEA LISA V. 8. *Kurva S: Jurnal Keilmuan Dan Aplikasi Teknik …*. http://ejurnal.untag-smd.ac.id/index.php/TEKNIKD/article/view/6413

Efendi, A. W. (2022c). Behavior of railroad bearing due to temperature and load using LISA FEA. *Journal of Railway Transportation and Technology*. https://jrtt.org/index.php/jrtt/article/view/1

Efendi, A. W. (2022d). Computing steel frame analysis of behavior semi-rigid connection. *International Journal of Advanced Science and …*. http://www.ijasca.org/index.php/ijasca/article/view/17

Efendi, A. W. (2022e). Structural Design Tuak River Pedestrian Suspension Bridge Anchor Block Type Rigid Symmetric with LISA. *Elektriese: Jurnal Sains Dan Teknologi Elektro*. https://jurnal.itscience.org/index.php/elektriese/article/view/1572

Efendi, A. W., Do, Y., & Rachman, N. F. (2022). Behavior of Rail Ballast Layer Using Mortar Foam with LISA-FEA. *Journal of Railway Transportation and …*. https://www.jrtt.org/index.php/jrtt/article/view/8

EFENDI, I. (2022). Noise exposure impact zone hue modeling using LISA FEA V. 8. *Teknik: Jurnal Ilmu Teknik Dan …*. http://journal.stiestekom.ac.id/index.php/TEKNIK/article/view/153

Efendi, I. A. W. (2022). Repair analysis of Pinang Bridge oprit subsidence with mortar form using LISA FEA V. 8. *Journal Of Research and Inovation in Civil …*. https://jurnal.politap.ac.id/index.php/rigid/article/view/786

Elsanadedy, H. M., Al-Salloum, Y. A., Alrubaidi, M. A., & ... (2021). Finite element analysis for progressive collapse potential of precast concrete beam-to-column connections strengthened with steel plates. *Journal of Building …*. https://www.sciencedirect.com/science/article/pii/S2352710220335087

Faridmehr, I., Tahir, M. M., Lahmer, T., & Osman, M. H. (2017). Seismic performance of steel frames with semirigid connections. *Journal of Engineering*.

FRAME, L. (n.d.). ДГКМ MASE. *Academia.Edu*.

Fumagalli, J., Pieroni, M., Renaux-Petel, S., & ... (2022). Detecting primordial features with LISA. *Journal of Cosmology …*. https://doi.org/10.1088/1475-7516/2022/07/020

Gullett, P. M., Dickey, M. M., & Howard, I. L. (2020). Finite Element Analysis of Highway Bridges Subjected to Hurricane Storm Surge via the AMBUSH Framework. *Journal of Bridge Engineering*. https://doi.org/10.1061/%28ASCE%29BE.1943-5592.0001602

Hindasageri, V., Kuntikana, P., Vedula, R. P., & ... (2015). An experimental and numerical investigation of heat transfer distribution of perforated plate burner flames impinging on a flat plate. *… Journal of Thermal …*. https://www.sciencedirect.com/science/article/pii/S1290072915000794

Jeyarajan, S., Liew, J. Y. R., & Koh, C. G. (2015). Analysis of steel-concrete composite buildings for blast induced progressive collapse. *International Journal of …*. https://doi.org/10.1260/2041-4196.6.3.457

Makarov, A. N. (2016). Calculations of Heat Transfer in Torch Furnaces by Gas Volume Radiation Laws. In *World Journal of Engineering and Technology*. scirp.org. https://www.scirp.org/html/13-1560323_70055.htm?pagespeed=noscript

Mashalkar, M. R. V, & Narkhede, M. T. (n.d.). Review on Dynamic Evaluation of Wind & Earthquake Forces Resisting Systems for Tall Building. In *Academia.edu*.

Mazzolani, F., Ricles, J. M., & Sause, R. (2009). *Behaviour of Steel Structures in Seismic Areas: STESSA 2009*. books.google.com.

McCormick, J., Fadden, M., & Buison, J. (2010). Cyclic testing of hollow structural sections for seismic applications in low to mid-rise moment frames. *Tubular Structures XIII*.

Nikoukalam, M. T., Mirghaderi, S. R., & ... (2015). Analytical study of moment-resisting frames retrofitted with shear slotted bolted connection. *Journal of Structural …*.

Okafor, V. C., Ogunoh, P. E., & Okechukwu, O. C. (2020). Finite Element Analysis of Fiber Cement Corrugated Roofing Sheet under Bending. *… Journal of Engineering and …*. https://ej-eng.org/index.php/ejeng/article/view/794

Qian, C. (2022). Mechanism of bacterial control of mineralisation gradient at the surface layer of cement-based materials. In *Advances in Cement Research* (Vol. 34, Issue 3, pp. 93–108). https://doi.org/10.1680/jadcr.21.00106

Shakeel, S., Fiorino, L., & Landolfo, R. (2020). Behavior factor evaluation of CFS wood sheathed shear walls according to FEMA P695 for Eurocodes. *Engineering Structures*.

Song, T., Liu, Y., & Wang, Y. (2017). Finite Element Method for Modeling 3D Resistivity Sounding on Anisotropic Geoelectric Media. In *Mathematical Problems in Engineering* (Vol. 2017, pp. 1–12). Hindawi Limited. https://doi.org/10.1155/2017/8027616

Tapes, C. (2020). *Cold-Formed Sigma Beams Retrofitted by Bonded*.

Taufik, S. (2008). *Behaviour of bolted connections with high strength and stainless steel*. search.proquest.com.

Trisni Bayuasri, Himawan Indarto, & Antonius. (2006). PERUBAHAN PERILAKU MEKANIS BETON AKIBAT TEMPERATUR TINGGI. *PILAR*, *15*(2).

Wang, Y. C., & Foster, A. (2017). Experimental and numerical study of temperature developments in PIR core sandwich panels with joint. *Fire Safety Journal*. https://www.sciencedirect.com/science/article/pii/S0379711217302540

Yang, R., & Zhou, X. (2019). Experimental Research and Theoretical Analysis of the Seismic Behavior of Prefabricated Semirigid Steel Frame with X-Shaped Braces. *Advances in Civil Engineering*.

Yuan, H., Hong, H. P., Deng, H., & Bai, Y. (2018). Displacement ductility of staged construction-steel tube-reinforced concrete columns. *Construction and Building Materials*.